Hindawi
Advances in Meteorology
Volume 2021, Article ID 9723676, 14 pages
https://doi.org/10.1155/2021/9723676

Research Article

Relationship between the Formation of $PM_{2.5}$ and Meteorological Factors in Northern China: The Periodic Characteristics of Wavelet Analysis

Yuanyuan Meng[1] **and Wanlong Sun**[2]

[1]*State Key Laboratory of Continental Dynamics, Department of Geology, Northwest University, Xi'an 710069, China*
[2]*Shaanxi Mineral Resources and Geological Survey, Xi'an 710068, China*

Correspondence should be addressed to Yuanyuan Meng; myychd@163.com

Received 11 July 2021; Revised 11 October 2021; Accepted 23 November 2021; Published 23 December 2021

Academic Editor: Marina Baldi

China's rapid urbanisation and industrialisation have led to frequent haze in China in recent years. Although many measures to control haze have been implemented, no significant improvement has been observed, and haze still exists. In this study, we used wavelet transform to investigate the changes in $PM_{2.5}$ on the time scale, the relationship amongst meteorological factors, and the causes and changes in haze formation and take measures to prevent haze. Results indicated the following: (1) The peak of $PM_{2.5}$ changes in winter in the past three years primarily occurred in the range from 11:00 to 13:00 and 20:00 to 22:00. (2) Multiple cycles of daily average $PM_{2.5}$ concentrations existed in 3–5 d, 6–14 d, 6–21 d, and 16–27 d, with a significant oscillation in 6–14 d and stable cycle characteristics. (3) The meteorological factors promoted the formation of haze to a certain extent. When haze occurred, the near-surface wind speed was only 1 m/s, which was not conducive to the spread of pollutants. (4) The formation of haze was affected by the interaction of various factors; the photochemical reactions of NO_2 and O_3 also exacerbated the formation of pollutants. This study provided a clear direction for the prevention and prediction of haze. Furthermore, the government must take relevant measures to reduce pollutant emissions and ensure the air quality of cities in winter.

1. Introduction

Air pollution is a major environmental risk factor affecting human health in developed and developing countries [1, 2]. $PM_{2.5}$ (particles with an aerodynamic diameter of $\leq 2.5\,\mu$m) is a fine particle that has been regulated in some countries such as the United States. China has also incorporated $PM_{2.5}$ into the draft amendments to the National Environmental Air Quality standards (Ministry of Environmental Protection of the People's Republic of China, 2011). The main feature of pollutants is the high concentration of their particles, resulting in a severe decline in visibility. At present, the prevention and control of air pollution in China are not only a topic in the field of atmospheric research but also a problem that the Chinese government and the public must solve [3–5]. The meteorological conditions restrict the area and long-term transport of air pollutants to a certain extent [6]. Under relatively stagnant meteorological conditions, the accumulation of $PM_{2.5}$ and the formation of secondary pollutants are also enhanced. Unfavourable meteorological factors may cause the formation and growth of new air pollutants and affect the dispersion of pollutants [7]. Severe air pollution during haze events is closely related to human emissions and local meteorological factors [8].The meteorological conditions are the main controlling factors for the occurrence of haze events and heavily polluted weather [9]. The meteorological conditions of an area primarily include natural factors, such as wind speed, wind direction, temperature, pressure, and humidity, which can affect the concentration of $PM_{2.5}$ in the air because these factors affect the dynamic conditions of air movement and particle propagation [10]. Moreover, the meteorological factors can be used as indicators to improve the estimated value of ground $PM_{2.5}$ concentration [11].

In recent years, the scope of meteorological station construction has been further expanded, and many remote areas have gradually improved with the establishment of monitoring stations. Pollutant data and some meteorological data are becoming public, and the number of people who study haze has also increased accordingly. Haze has become a hot research topic, which has attracted the attention of many scholars. Scholars used different methods to study the formation of haze and the law of spatial change and focused on establishing different haze prediction models. They have designed an empirical model to predict the daily average concentrations of $PM_{2.5}$ and PM_{10} in future London pollutants [12]. However, the autoregressive integrated moving average is used to determine PM_{10} trends in traffic pollution in Hangzhou [13]. Some scholars have collected PM_{10} concentrations at 27 sites in Beijing to investigate the spatiotemporal characteristics of PM_{10}, and the results showed changes in PM_{10} concentrations in different seasons and at different sites [14]. Most of the previous studies have focused on the occurrence of haze at a long-term scale as a whole, which had little effect on small-scale studies. The formation of haze is multiscale and multifactor, and the main factors affecting its formation must be comprehensively analysed.

In addition to the meteorological factors, the formation of severe haze causes severe pollution. Studies have shown that weather conditions on the ground are not the only factors affecting the formation of air pollution [15]. Adverse weather conditions, excessive emissions of pollutants, and secondary conversion of pollutant particles are also the main causes of severe pollution [16]. Haze, which is a secondary pollutant, has contributed greatly to severe weather, and aerosols have an important impact on the amount of radiation, visibility, and air quality of the Earth on a regional and global scale [17]. Secondary organic aerosol (SOA) is formed by the gas-phase oxidation reaction of living organisms and the gas-phase oxidation reaction of man-made volatile organic compounds with ozone (O_3), hydroxyl (OH), and nitrate (NO_3). The formation of secondary pollutants greatly contributes to haze. Although scholars have studied considerable $PM_{2.5}$, they have little research on the local time scale. The evolution of $PM_{2.5}$ is not stable, and many factors affecting the trend of $PM_{2.5}$ are found. Therefore, this study aimed to investigate the overall $PM_{2.5}$ and part changes. The local evolution of $PM_{2.5}$ was studied using wavelet transform, and the cause of local $PM_{2.5}$ pollution and its relationship with meteorological factors were discussed.

We are also concerned about the evolution characteristics of $PM_{2.5}$ in severe haze days and make prediction measures for the subsequent haze events. We collect data on various pollutants and meteorological factors during the severe haze period to comprehensively analyse the causes of localized haze and better understand the trends of pollutants during the severe haze period.

2. Data and Methods

2.1. Data Sources. Weinan (34.14 N, 109.43 E) is located in the eastern part of the Weihe Plain in Guanzhong, Shaanxi Province, with approximately 5.359 million residents (National Bureau of Statistics of China https://data.stats.gov.cn/easyquery) and a total area of approximately 13,134 km^2. It is the largest agricultural city and the second largest city in Shaanxi Province. The climate is dominated by a temperate continental monsoon. Weinan is adjacent to the Qinling Mountains to the south and the Loess Plateau to the north. The regional geographic information of the study area is shown in Figure 1.

The research data presented in this article were obtained from real-time monitoring data released by the China National Environmental Monitoring Centre (https://www.cnemc.cn). Considering that the winter haze phenomenon was relatively serious, the article studied the relationship between winter haze and meteorological factors; therefore, the data were primarily recorded in winter. Four automatic monitoring stations were identified: Gao Xinyi Xiao, Gymnasium, Daily Newspaper Office, and Agricultural Science Institute (Table 1 and Figure 2).

We obtained about 1,050 daily average $PM_{2.5}$ concentration readings from January 2014 to February 2016 from each station. At the same time, the missing data has been replaced by the mean of the two nearest data. Given the failure of the monitoring station, contaminant data ($PM_{2.5}$, SO_2, CO, NOX, and O_3) were not recorded at some time, and the data were missing. The missing data has been replaced by the mean of the two nearest data. Meteorological data (such as temperature, humidity, and wind speed) were obtained from Weather Underground (https://www.wunderground.com/hurricane). Hourly $PM_{2.5}$concentration data were obtained from the official website of the China Environmental Monitoring Centre (CEMC: https://106.37.208.233:20035). In addition, we also obtained digital elevation model (DEM) data with a resolution of 90 m in the Weinan area from the Geospatial Data Cloud (https://www.gscloud.cn/).

Given the effect of topographical factors in the Weinan area and that the wind direction rarely changed, the wind speed was low, and the frequency of still wind was high. Thus, the formation of pollutants was relatively stable, which was suitable for multiscale time analysis. The factors related to pollutant formation in Weinan City were relatively stable; therefore, studying the changes in haze pollutant concentration on multiple time scales was suitable. Studies have shown that the multiscale characteristics of $PM_{2.5}$ in various time evolution processes cannot be ignored, and they might play an important role in predicting haze [18].

Considering that the factors related to the formation of local haze were complicated, we selected the most severe haze period as the research object. January 2016 was one of the periods with severe haze; thus, this period was used to study intermittent local periodic changes. We primarily conducted time-scale research on the data collected in January 2016. Moreover, the daily variation characteristics of $PM_{2.5}$ in the winter of 2014 to 2016 were analysed. Furthermore, meteorological and pollutant data from January 1, 2016, to January 10, 2016, were selected for analysis.

2.2. Methods. In recent years, wavelet transform has been used by several researchers for time-scale transformation [18]. Wavelet analysis was firstly applied to the analysis of

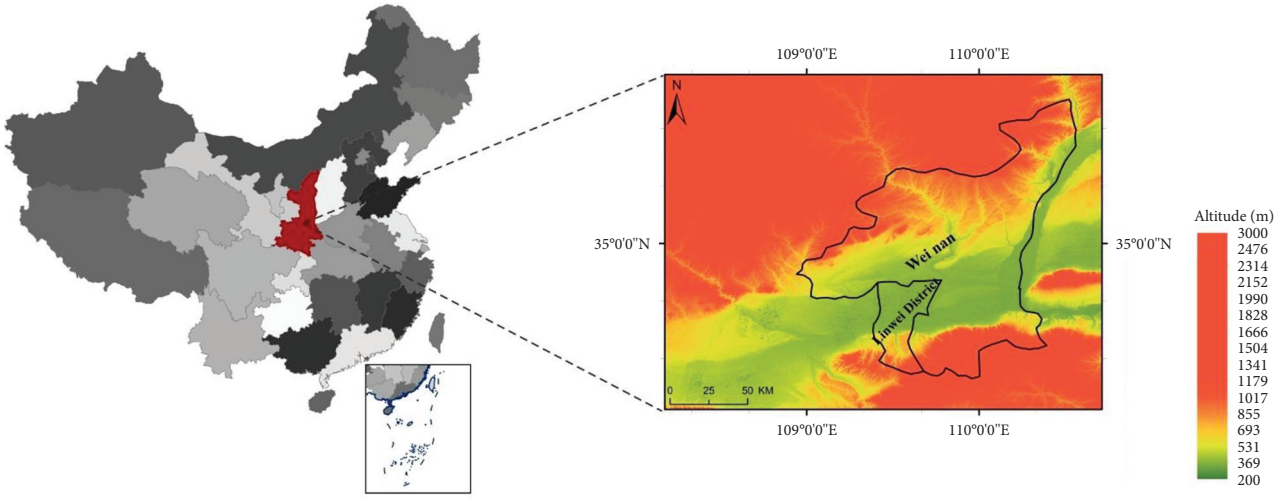

Figure 1: Regional geographic information of the study area.

Table 1: Air quality monitoring station in Weinan.

Station number	Station name	Latitude/degree (N)	Longitude/degree (E)
1	Agricultural Science Institute	34.51	109.53
2	Daily Newspaper Office	34.50	109.50
3	Gymnasium	34.49	109.46
4	Gao Xinyi Xiao	34.50	109.43

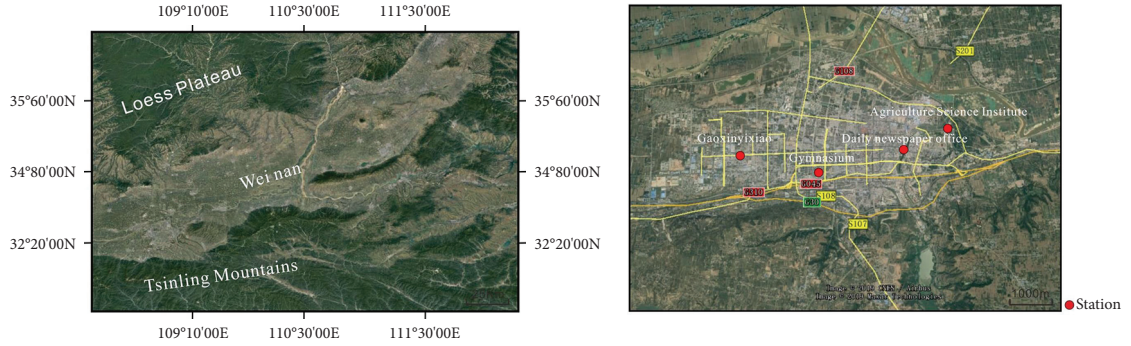

Figure 2: (a) Topographic map of the Guanzhong Basin; (b) distribution of four monitoring stations in Weinan.

seismic signals [19]. At present, wavelet analysis has been widely used in science, engineering, mathematics, and other fields, particularly in geophysics [20]. Wavelet transform analysis is an effective tool for studying the power spectrum transformation in the time scale. It could effectively reveal the main transformation trends and the changing of these trends in the time range. The time series is decomposed into the time-frequency space. Wavelet transforms have two main types: discrete wavelet transform and continuous wavelet transform. The discrete wavelet transform was used for signal compression and signal denoising [21]. By contrast, the continuous wavelet transform was widely used in geophysical research to extract intermittent wave signals in time [22]. This paper primarily used the continuous wavelet transform (CWT) to study the time variation characteristics of $PM_{2.5}$. Taking the time series of $PM_{2.5}$ concentration x_n, the time interval δt is equal, $n = 0,\ldots N-1$ and the mother wavelet ψ (t), which depends on a dimensionless 'time' parameter t. To satisfy the admissibility condition, $\psi(w)|_{w=0} = 0$ and ψ (t) must have zero mean and be located in time and frequency space [23]. The continuous wavelet transform of the discrete sequence x_n is defined as the convolution of x_n and the subwavelet, which are the translated and scaled version of the mother wavelet ψ (t):

$$w_n^x(S) = \sqrt{\frac{t}{s}} \sum_{n'=0}^{N-1} x_{n'} \psi * \left(\frac{(n'-n)t}{S} \right),$$
$$C\psi = \int_{-\infty}^{+\infty} \frac{|\psi(w)|2}{|w|} \mathrm{d}w < \infty, \tag{1}$$

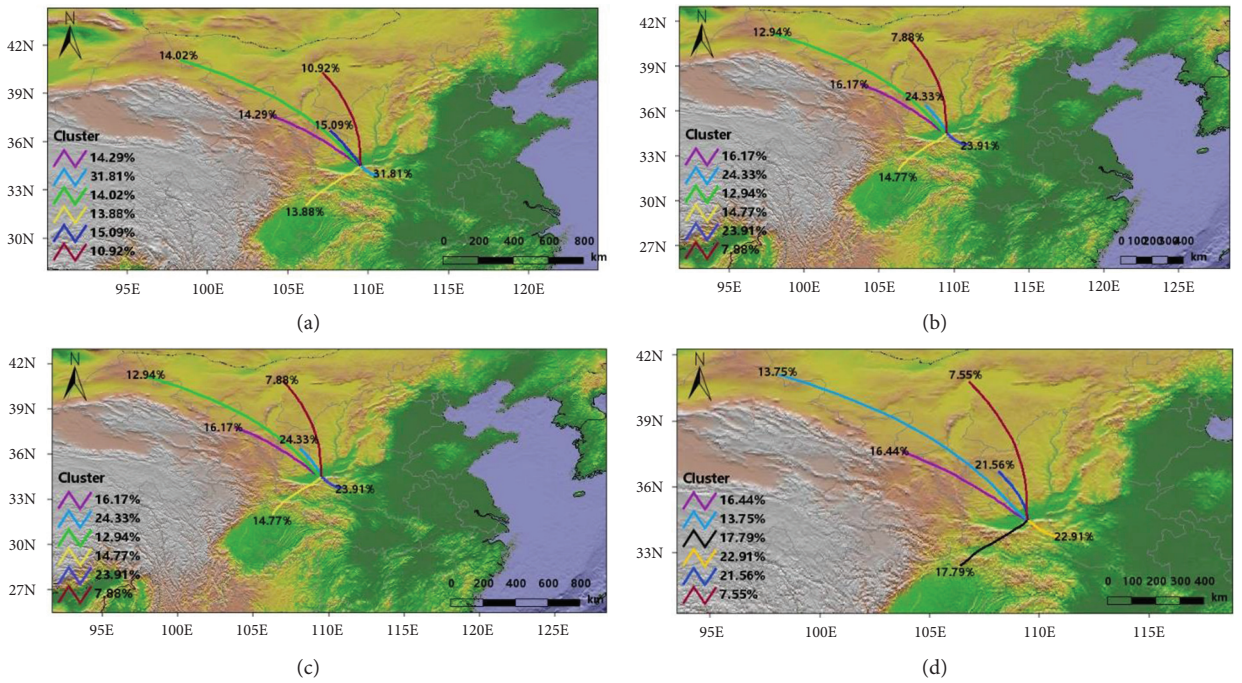

Figure 3: (a–d) The backward trajectory distribution characteristics of four monitoring stations: Agricultural Science Institute, Daily Newspaper Office, Gymnasium, and Gao Xinyi Xiao.

where (*) represents a complex conjugate. W_n, and $X(s)$ is also called wavelet coefficient, which represents the correlation between wavelet and data array. Both the wavelet scale s and the localized time index n are continuous real numbers. The larger the wavelet scale s, the wider the $\psi(t/s)$, and the signal characteristics are more obvious on the multiscale of the original signal. By changing the wavelet scale s and shifting along the local time index n, an image can be constructed to show the relationship between the amplitude of any feature and the scale and how the amplitude changes over time.

In this paper, to retain both the amplitude and phase information of the $PM_{2.5}$ concentration sequence signal, Morlet wavelet is selected as the mother wavelet. It is a single-frequency complex sine function with symmetry, nonorthogonality, and imaginary part, which can express phase information well [24] as follows:

$$\psi(t) = (\pi \times f_b)^{-1/2} e^{2i \times fc \times t} e^{-t^2/f_b}. \quad (2)$$

In (2), t represents time and f_b represents the bandwidth for controlling the attenuation in the time domain and the corresponding bandwidth in the frequency domain. f_b is the reciprocal of the variance in the frequency domain. The increase of f_b will make the wavelet energy concentrate near the center frequency and slow down the decay speed in the time domain. Conversely, a decrease in f_b will accelerate the decay rate in the time domain and reduce the energy in the frequency domain. fc represents the center frequency, and the value of the frequency will be affected when the time domain is converted to the frequency domain. $\psi(t)$ is a complex Morlet wavelet determined by f_b and f_c.

3. Results and Discussion

3.1. Characteristics of Daily Mean Value of $PM_{2.5}$ in Winter from 2014 to 2016. We averaged the 24 h real-time concentration of $PM_{2.5}$ in the winter of 2014–2016. Considering that the annual change values that we often used were composed of $PM_{2.5}$ concentration values per hour, we analysed the overall change trend from a macro perspective. The changes in $PM_{2.5}$ values during the three winter years were analysed to understand the time change characteristics of $PM_{2.5}$. As can be seen from the backward trajectory distribution map (Figure 3), the pollutant transport trajectories are similar at the four monitoring site locations. Therefore, using the average of the four stations better reflects the local distribution of pollutants. The percentages of air masses in northwestern China are 54.2%, 60.87%, 61.32%, and 59.3%, respectively. The CWT model results in Figure 4 suggest that long-range transport was the main contributor to $PM_{2.5}$ in Weinan. The most polluted air masses are mainly from southern Shaanxi and northern Chongqing. Inner Mongolia, Gansu, and Ningxia are also potential sources of $PM_{2.5}$.

As can be seen from Figure 5, the comprehensive 24-hour variation characteristics of $PM_{2.5}$ concentrations during the winter period from January 2014 to February 2016 show that there are two obvious peaks in $PM_{2.5}$ concentration values, which occur at 11:00–13:00 and 20:00–22:00, respectively. During the period 2014.1–2016.2, the overall trend is that the $PM_{2.5}$ concentration gradually increases after 8:00, mainly because the morning peak of the day starts at this time when the solar radiation is enhanced, the temperature rises, people start to go out and carry out their activities, and motor vehicle

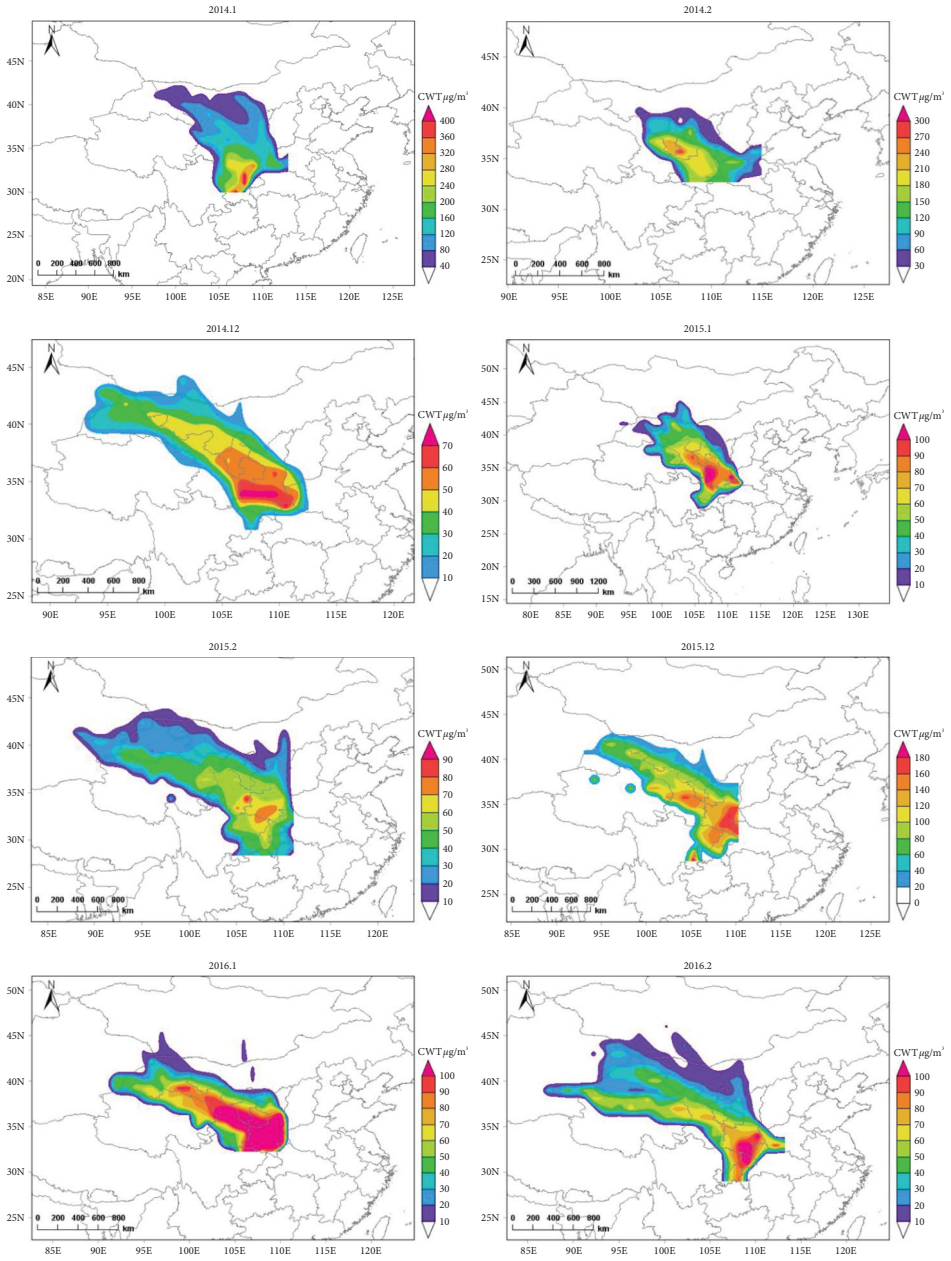

Figure 4: Concentration-weighted trajectory distribution of $PM_{2.5}$ in Weinan from January 2014 to February 2016.

exhaust increases rapidly. The period from 11:00–13:00 is the peak time for leaving work, human activities increase, motor vehicle emissions increase, and $PM_{2.5}$ concentrations increase during this period. After 14:00, people's outdoor activities decrease, and due to the urban heat island effect, the urban area warms up quickly, and the airflow forms a local circulation from the suburbs to the urban area, which promotes the diffusion of pollution particles. Studies have shown that the urban heat island effect is influenced by a combination of meteorological conditions, the nature of the subsurface, and anthropogenic heat emissions [25, 26]. The urban heat island effect has many negative effects, such as increasing the degree of heat waves in summer [27], increasing energy consumption and greenhouse gas emissions for cooling in summer [28], increasing air pollution, and decreasing urban livability [29], which is not conducive to the sustainable development of the ecosystem. In the evening, with the arrival of the evening peak and the active urban dining and entertainment activities, the concentration of pollutants gradually increased. At this time, the surface temperature of the lower layer of the city drops, and it is lower than the upper atmosphere, forming an inversion layer, which hinders the diffusion of pollutants. Therefore, the evening peak appears during 20: 00–22: 00. Based on the above-mentioned analysis, the peak value of $PM_{2.5}$ change in winter in three years primarily occurred at 11: 00 to 13:00 and 20:00 to 22:00. The general trend is that the $PM_{2.5}$ concentration gradually increases after 8;00, and 11: 00–13:00 is the peak period of work, human activities increase, and motor vehicle exhaust emissions increase. After 14:00, people's outdoor activities are reduced, and due to the urban

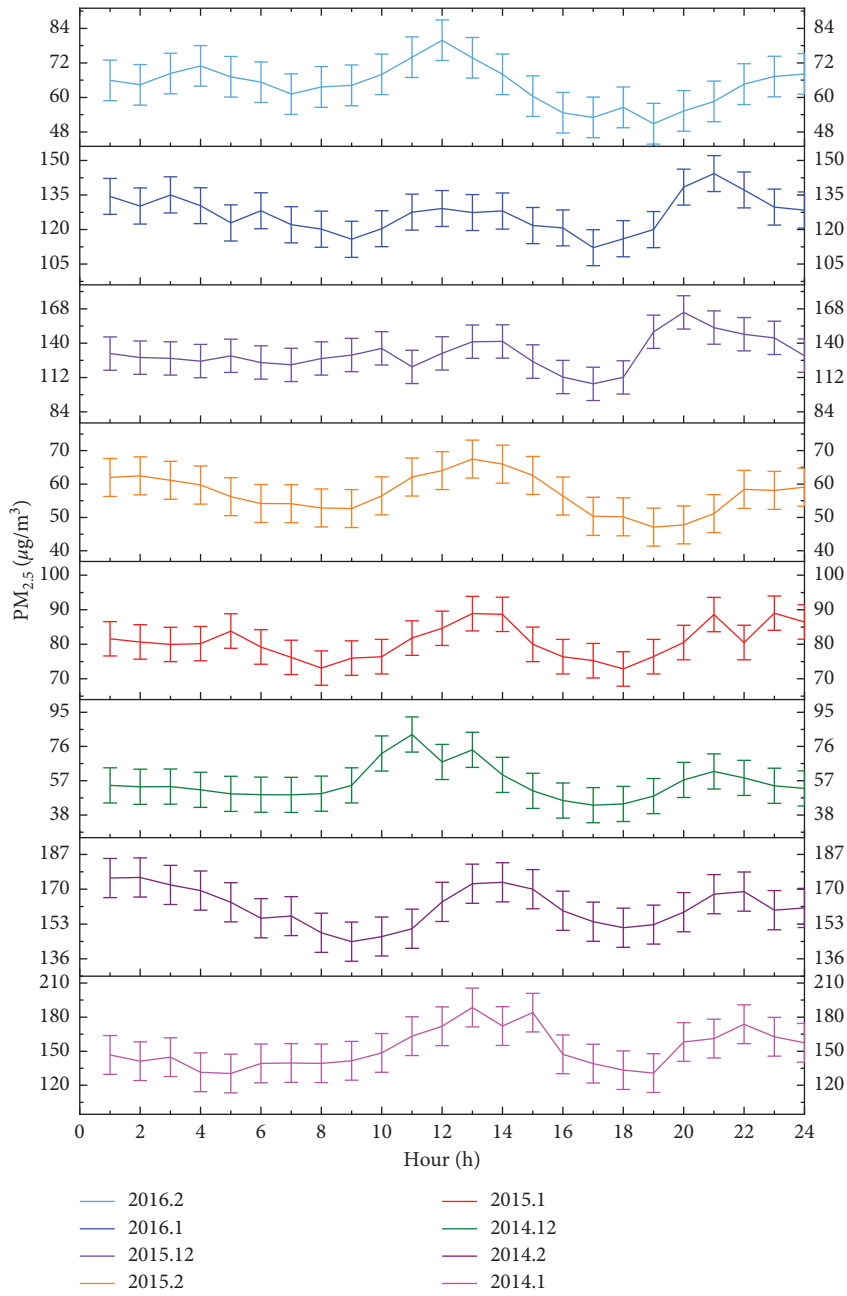

Figure 5: Time series trend of 24 h real-time concentration change of $PM_{2.5}$ in winter from January 2014 to February 2016 (the vertical bar represents the standard deviation).

heat island effect, the urban area heats up rapidly, and the airflow forms a local circulation from the suburbs to the urban area, which promotes the diffusion of pollutant particles. In the evening, influenced by the dining and entertainment activities in the urban area, as well as the rapid decline in the temperature of the lower cushion surface of the urban area, it is easy to form an inverse temperature, the diffusion of pollutants is blocked, and the evening peak occurs at 20:00–22:00.

3.2. Monthly Real-Time Concentration of $PM_{2.5}$. The severe winter haze was used as the monthly change of $PM_{2.5}$ to determine the occurrence of severe haze in the future. As shown in Figure 6, where the horizontal axis represents the time in the unit of day and the vertical axis represents the wavelet scale. There exist distinct scales of variation of the $PM_{2.5}$ concentration in the entire time domain, which can provide us with an overall cognition of the variation trend to predict further changes. If the region of the contour map is filled with a warm color, the real part is positive, which means that the air quality of Weinan is poor, and the haze pollution is serious. If the filling color is cold, the real part is negative, indicating that the air quality in Weinan is good, and the haze pollution is slight.

Figure 6 shows that there are multiple periods of the daily average $PM_{2.5}$ concentration, which are on the scale of

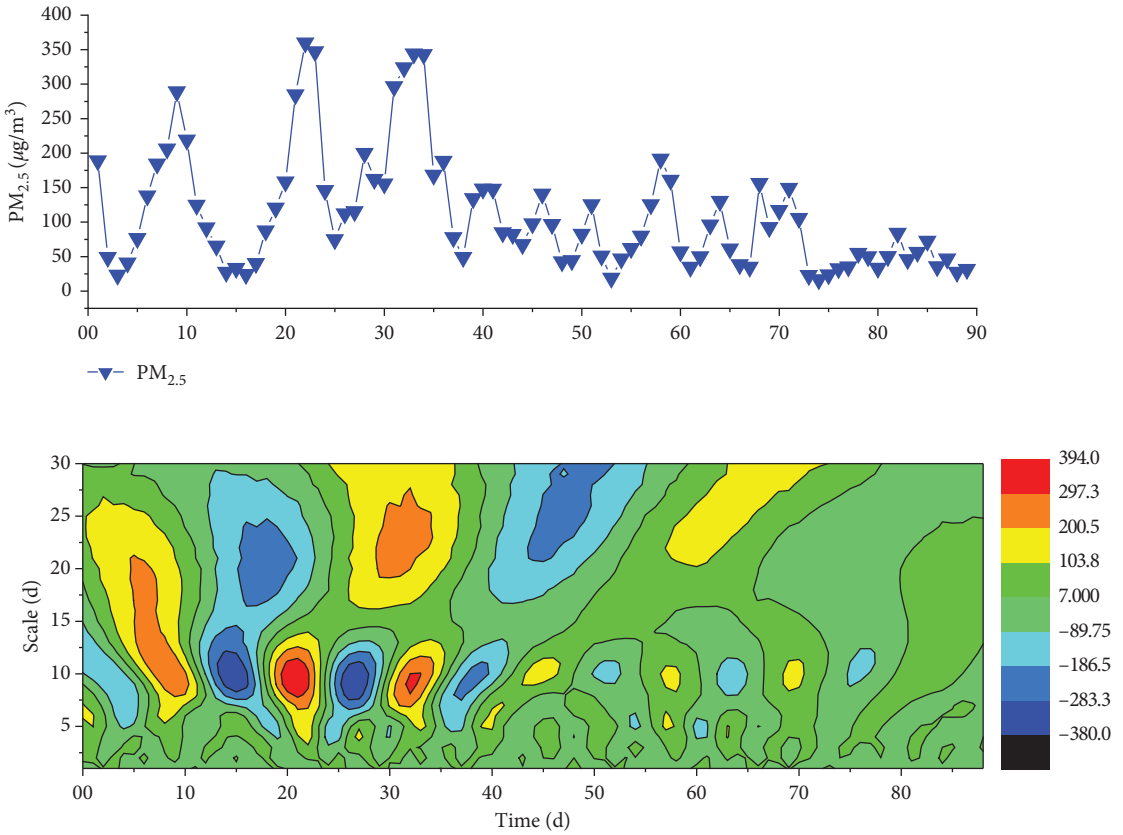

Figure 6: The real part of wavelet coefficients $R\{WnX(s)\}$ in three months. The horizontal axis represents time in the unit of day and the vertical axis represents the scale in the unit of day.

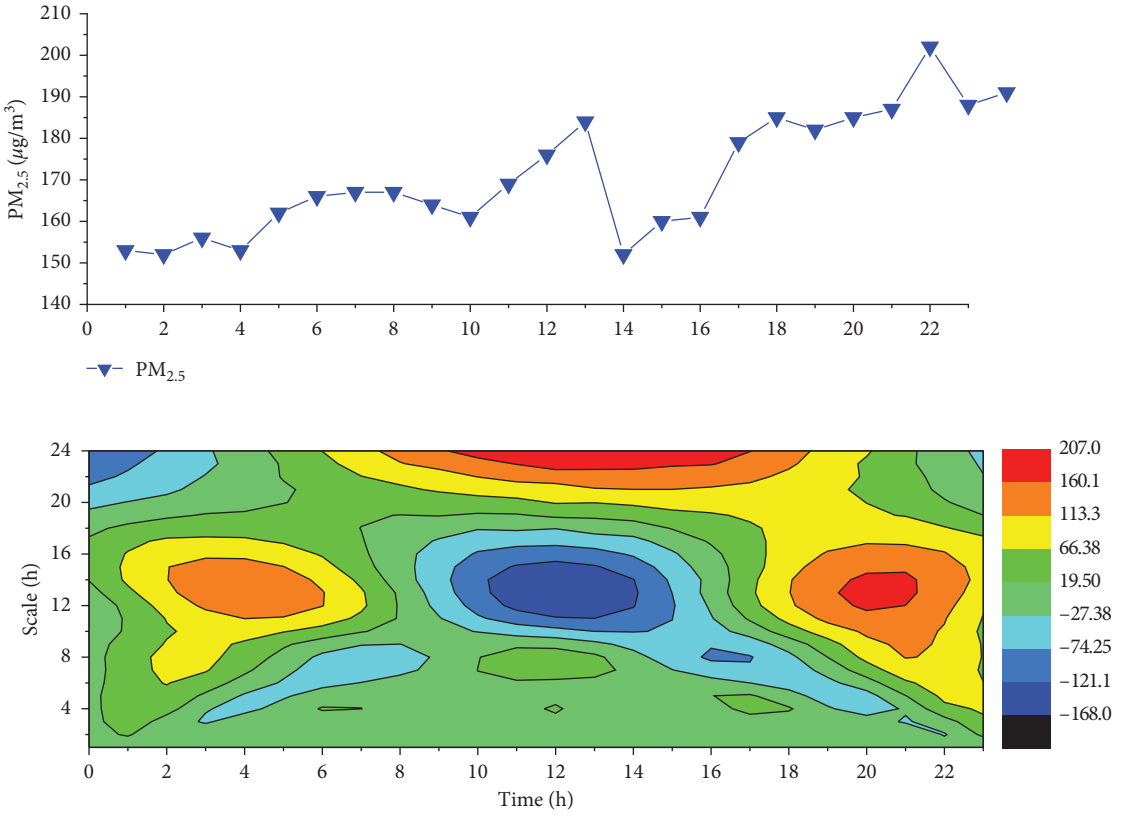

Figure 7: Daily time series of $PM_{2.5}$ and the real part of the wavelet coefficient $R\{Wn, X(s)\}$ in one day. The horizontal axis represents time in hours, and the vertical axis represents the conversion scale in hours.

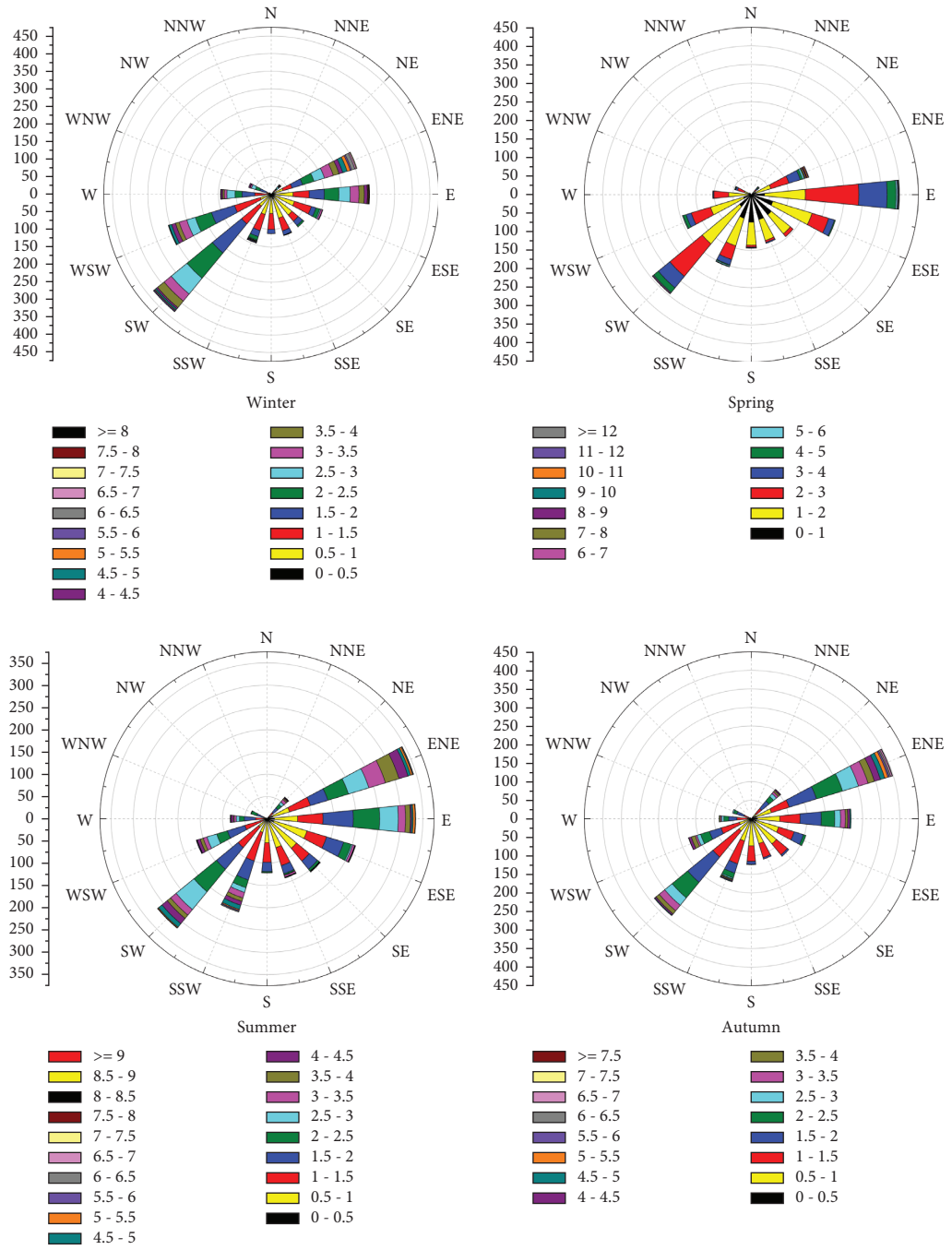

Figure 8: Relationship between wind speed and direction in Weinan area from December 2014 to November 2015 (winter, spring, summer, and autumn, resp.).

3–5 d, 6–14 d, 6–21 d, and 16–27 d. In particular, there are obvious oscillations on the scale of 6–14 d, and the periodic characteristics are stable. There is a dominant oscillatory period of 6–14 d in the evolution of daily $PM_{2.5}$ concentration, which is the convergence of several small oscillation periods. In the entire time domain, there are three warm centers in 7 d, 21 d, and 32 d, respectively, during the winter, the period with serious haze pollution; two cold centers occur on 15 d and 26 d, corresponding to the absence or presence of slight haze pollution. The energy distribution shown in Figure 6 reveals good conformity with the realistic conditions. Prevention should be done before the next haze occurs. The frequency of haze pollution was closely related to local meteorological factors and human activities.

3.3. Real-Time Concentration Change Characteristics of $PM_{2.5}$ in 24 h. Based on the hourly changes (Figure 7), the $PM_{2.5}$ value was the highest at night; the concentration value was 205 $\mu g/m^3$. The concentration value at noon was 185 $\mu g/m^3$. The subpeak value appeared around 3 am. There are two apparent periodic changes during the evolution of $PM_{2.5}$

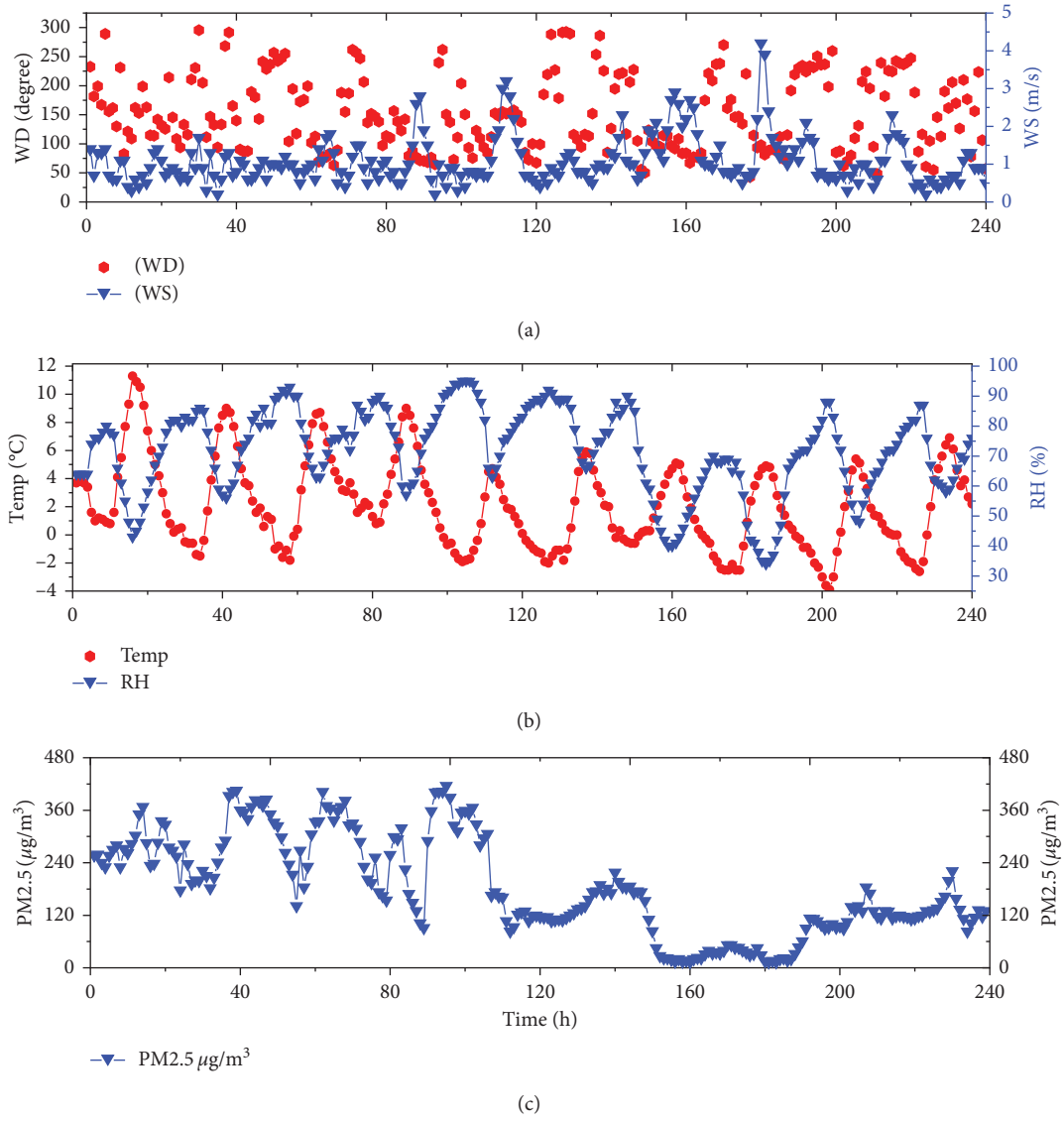

Figure 9: Time series of meteorological parameters and pollutants from January 1 to 10, 2016. (a) WD: wind direction; *WS*: wind speed (m/s); (b) Temp: temperature (°C); RH: relative humidity (%).

concentration, on the scale of 10–18 h and 20–24 h. $PM_{2.5}$ has two obvious periodic changes in the evolution, especially in the scale of 10–18 h, with three oscillatory processes, and the periodic characteristics are relatively stable in the whole time domain. The warm center is distributed around 12 h and 21 h; the cold center is distributed around the 1 h and 14 h. The real-time concentration of $PM_{2.5}$ varied from day to day, but it was more consistent at several important pollution nodes. Several time points, when $PM_{2.5}$ appeared severely polluted, were within the predicted time range. Therefore, using a certain day was feasible to study the hourly change of real-time $PM_{2.5}$ concentration value. As the rush hours primarily occurred in the morning, the city's traffic emissions within this range increased. In recent years, the number of highway vehicles in China has increased rapidly. Vehicle emissions have a great impact on daily air. The high $PM_{2.5}$ value at night was primarily due to traffic pollution during rush hours and fumes from the catering industry. In addition, electricity prices were low at night. Some factories conducted industrial production at night to reduce costs, resulting in increased pollutant concentrations at night. This result eventually led to $PM_{2.5}$ peaks from night to early morning, which was also related to meteorological factors.

3.4. Meteorological Conditions and Pollutant Concentrations. Weather conditions play a vital role in the daily fluctuations of air pollutants [30]. To date, many studies have focused on the physical and chemical properties of pollutants [5, 31], and few studies have quantitatively explored the relationship between air pollutant concentrations and meteorological conditions [30].The concentration of haze depends on wind speed and humidity to a certain extent.

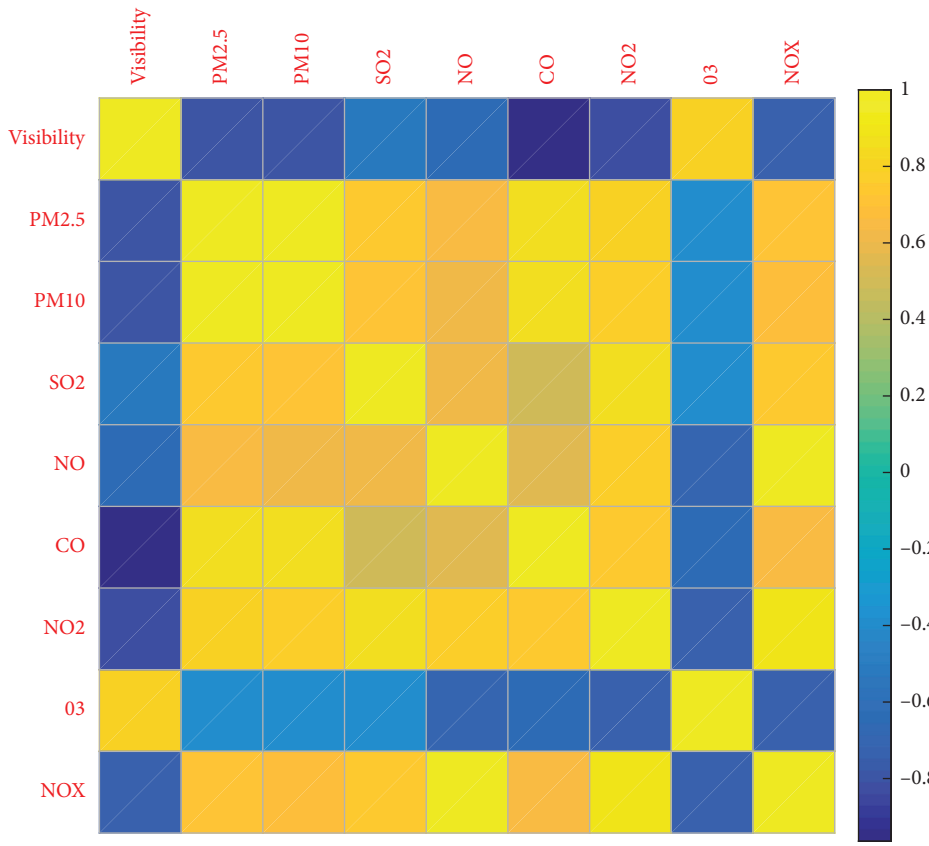

Figure 10: Spearman correlation between real-time monitoring visibility data and each pollutant factor was shown from January 1 to January 10, 2016 (the darker the color of the square, the stronger the correlation).

Wind speed is related to the transport and diffusion of pollutants, and humidity is related to air hygroscopicity and scattering [16].

We show the wind direction and wind speed data from December 2014 to November 2015 to produce wind rose diagrams for different seasons: winter, spring, summer, and autumn, respectively. As shown in Figure 8, the wind direction is almost dominated by northeast-southwest winds in all four seasons. The northeast wind direction occurred most frequently, followed by the southwest wind direction. The maximum wind speed in the spring exceeds 12 m/s, and the larger wind speed is beneficial to the diffusion of pollutants. However, when dust storms occur, larger wind speeds can also lead to an increase in $PM_{2.5}$ concentrations [32]. Conversely, lower wind speed is not conducive to the diffusion of pollutants but makes the mixing of pollutants more adequate and provides conditions for secondary reactions of particulate matter, which intensifies the increase of particulate matter concentration [33]. In addition, the wind direction determines the diffusion direction of particulate matter, which also has an impact on $PM_{2.5}$ concentration.

This study found that the areas with low winter wind speeds were primarily mountainous or transitional areas between plains, where haze was generally serious. Therefore, *SW* or *W* winds in the lower troposphere were conducive to the accumulation of air pollutants, and weaker surface winds might weaken the dispersion of pollutants [34]. As shown in Figure 9, the surface wind speed during haze events was weak, and the wind speed appeared more frequently at 1 m/s. Studies have shown that when the wind speed is 1 m/s, it is not conducive to the diffusion of pollutants [31]. The wind direction and wind speed in Weinan City are not conducive to the diffusion of pollutants when haze occurs.

An increase in temperature would increase the concentration of pollutants. The updraft caused by the warm temperature would force the air near the ground to move upwards, which would cause low pressure in local areas. Clouds could be generated by humid updrafts. Therefore, moving in the vertical direction and dispersion would be difficult for air pollutants. High humidity was also conducive to the nucleation, coagulation, and solidification of submicron particles and stable stratification in the boundary layer with low mixing layer height [35–37]. RH had a crucial effect on the chemical composition, size distribution, and optical properties of aerosol particles [38, 39]. In addition, RH affected aerosol formation in different ways [42].

3.5. Visibility Conditions. The results showed that the low visibility under low RH conditions was due to the heavy aerosol load, whereas, under high RH conditions, the hygroscopic growth of aerosols would become strong, leading to low visibility events even at moderate aerosol pollution

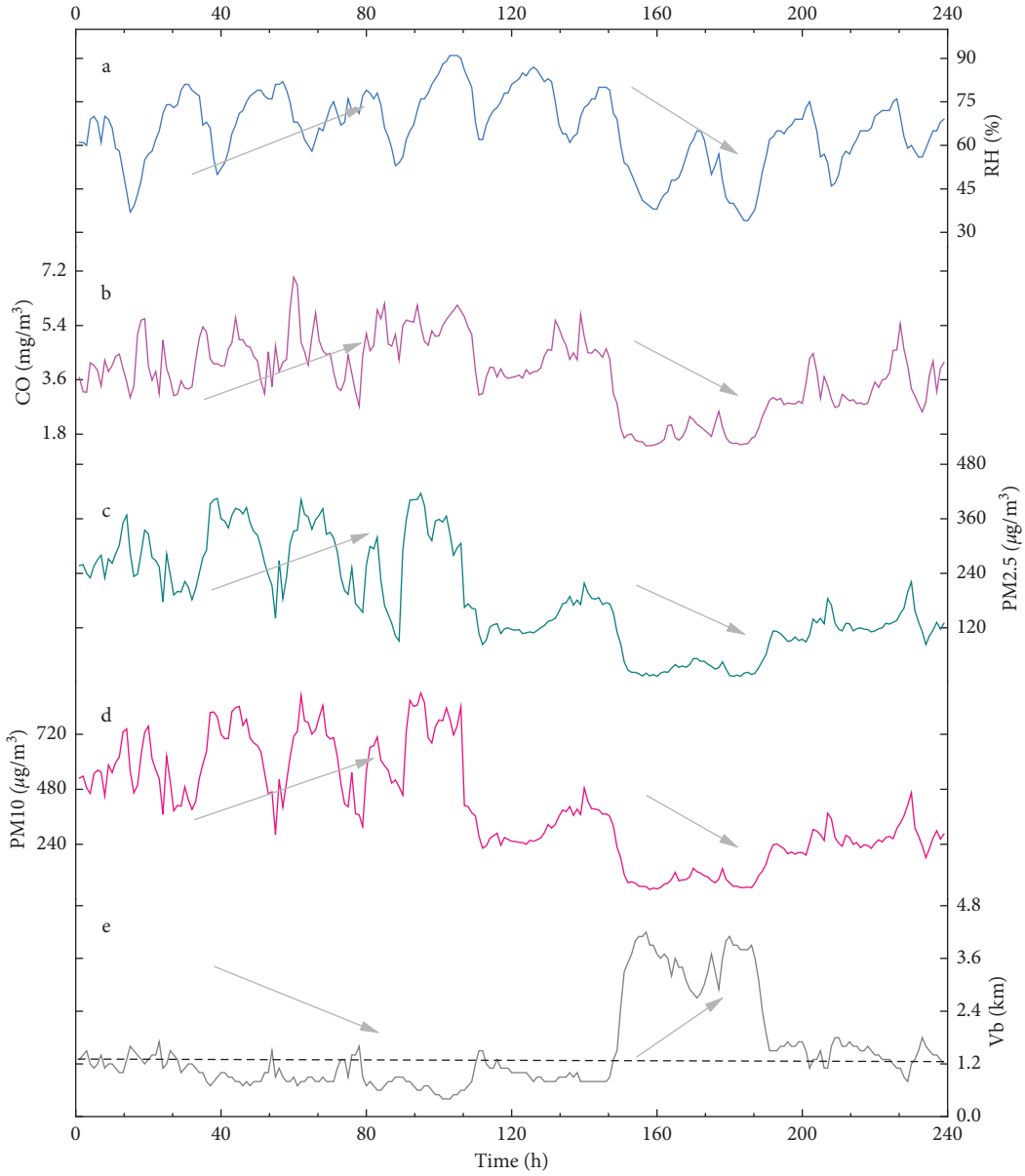

Figure 11: Time series of visibility and each pollutant from January 1 to 10, 2016. (a) RH: relative humidity (%); (b) CO (mg/m^3); (c) $PM_{2.5}$ (μg/m^3); (d) PM_{10} (μg/m^3).

levels [3]. Heavy fog and severe haze events have dramatically reduced visibility, resulting in a heavy burden on air transportation and road traffic, and seriously endangered the lives of citizens. In addition, severe aerosol pollution had a high degree of damage to human health, leading to decreased visibility [3]. Visibility was also affected by meteorological factors, that is, visibility increasing with temperature and wind speed, whereas RH and atmospheric pressure decreased [5]. Daytime visibility was defined as the distance an ordinary observer could barely distinguish between the outline of a black object and the horizontal skyline. In a clean atmosphere, the normal range of visibility was 145 km to 225 km [41]. The aerosol load was high enough to eliminate the light and cause low visibility. As hygroscopic aerosol particles increased in RH, they reduced visibility, particularly at night [42].The rapid increase in aerosol load in the surface and vertical distribution was primarily due to regional transport, which severely affected visibility [42]. However, research showed that the low visibility of the contaminated sites was primarily due to the increase in the concentration of artificial aerosol particles [43].

Therefore, this paper used Spearman correlation to analyse the correlation between visibility and major pollutants. Figure 10 shows the Spearman correlation between real-time monitoring visibility data, and each pollutant factor was shown from January 1 to January 10, 2016. Spearman correlation was used to analyse the correlation between visibility and major pollutants. The color of the square indicates the size of the correlation coefficient, and the darker the color, the stronger the correlation (otherwise the weaker). Correlation analysis was performed on pollutants and visibility from January 1, 2016, to January 10,

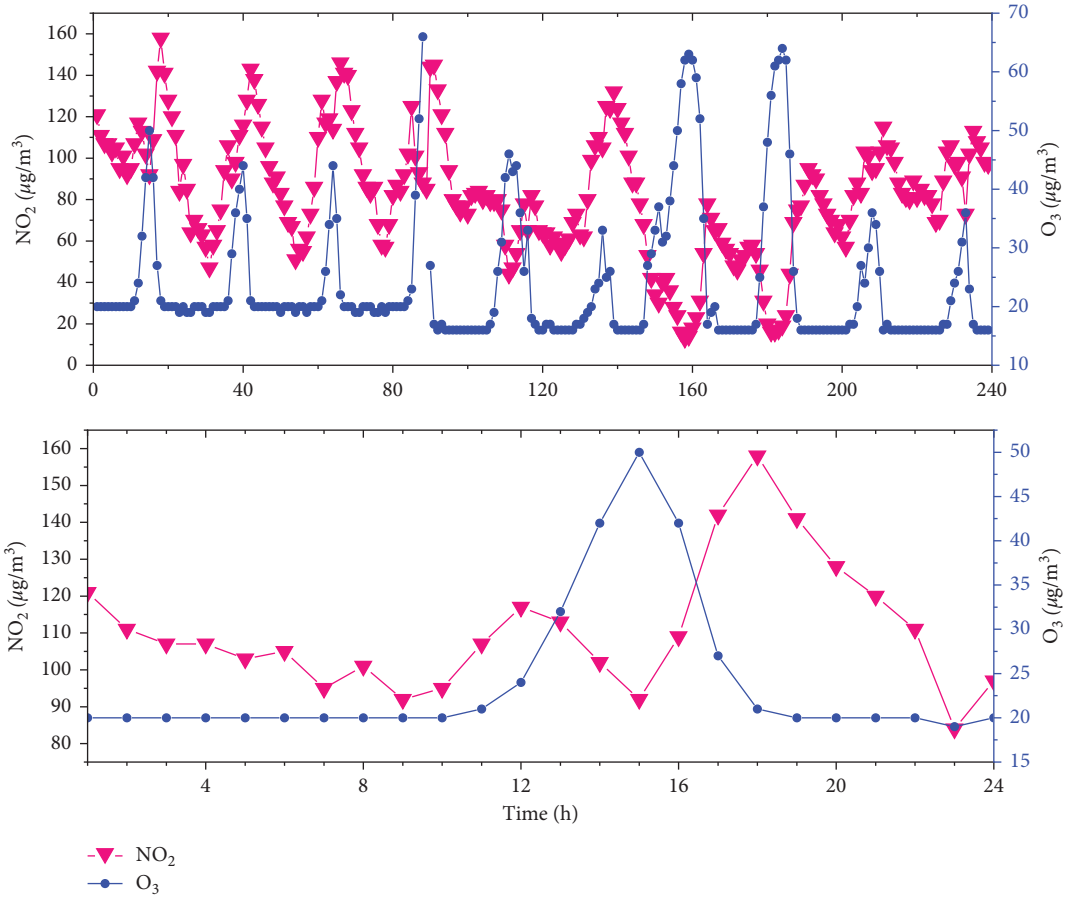

Figure 12: Time series of daily and hourly trends of NO_2 and O_3 from January 1 to 10, 2016.

2016. Figure 10 showed that visibility was negatively correlated with $PM_{2.5}$ and PM_{10}.

Moreover, a certain correlation was observed between visibility and SO_2, as well as CO and NO_2. The visibility was greatly affected by the main pollutants. However, wind speed also had a great impact on visibility. Most wind speeds during the severe haze period were only 1.0 m/s, and pollutants were accumulated locally (Figure 9(b)). The concentration of pollutants rose sharply, whereas the secondary pollution intensified.

Time series analysis was performed on the pollutant data from January 1, 2016, to January 10. Figure 11 shows that, during the first 144 h of severe pollution, the PM_{10} trend was rising, and visibility was on the decline. Furthermore, RH promoted the accumulation of pollutant concentrations when the haze was severe, and the combined effect of these factors led to a sharp decline in visibility. However, between 144 and 186 h, the RH, CO, $PM_{2.5}$, and PM_{10} showed a downward trend and increased visibility caused by the increased wind speed when the cold air comes and blew off the pollutants. As shown in Figure 9(a), the wind speed increased between 140 h and 190 h.

3.6. Relationship between O_3 and NO_2. O_3 pollution is the product of photochemical reactions of its precursors nitrogen oxides (NOx) and volatile organic compounds (VOCs) in the presence of ultraviolet light [44, 45]. The increase in O_3 concentration can cause serious harm to human health. Therefore, the control of O_3 pollution is the key object of prevention and control required for the continuous improvement of atmospheric environmental quality and ecological civilization construction in China in the next phase. As shown in Figure 12, NO_2 and O_3 showed evident daily changes. The diurnal variation of NO_2 has two crests: the first one at around 12:00 and the second at around 18:00. The daily change cycle of O_3 has an evident peak during the day (15:00), whereas the value of the other pollutants in the morning and evening does not change significantly, and the concentration continues at 20 ($\mu g/m^3$), indicating that the level of O_3 during the day is different. Furthermore, the concentration has decreased at night. The O_3 concentration reaches its highest value around 15:00 as the temperature rises and solar radiation continues to intensify from the morning, after which the photochemical reaction rate slows down and is lowest at night, which is typical of photochemical reactions. This has been corroborated in several studies [46, 47].

4. Conclusions

We used Morlet wavelet transform to analyse the daily and monthly changes of $PM_{2.5}$ in winter, which are the daily real-

time $PM_{2.5}$ concentration change characteristics and hourly $PM_{2.5}$. Three months of winter $PM_{2.5}$ data are selected for the study. Considering that the change characteristics of $PM_{2.5}$ are nonuniform, we use the hourly scale to study the change rules accurately and provide a basis for us to determine the occurrence and prevention of haze.

The daily average $PM_{2.5}$ concentration has several periods, 3-5 d, 6–14 d, 6–21 d, and 16–27 d, of which 6–14 d has a clear oscillation with stable period characteristics. In the evolution of daily $PM_{2.5}$ concentrations, there is a dominant oscillation period at 6–14 d, which is the confluence of several small oscillation periods. In the whole time domain, there are three warm centers appearing at 7 d, 21 d, and 32 d, which are periods of severe haze pollution in winter, and two cold centers appearing at 15 d and 26 d, corresponding to periods without or with slight haze pollution.

Strong temperature inversion, weak ground wind speed, and falling air movement cause pollutants to accumulate in the shallow layer, and pollutants accumulate in the area because of adverse meteorological conditions. Additionally, adverse meteorological conditions, such as the presence of RH, have caused the increase of $PM_{2.5}$ concentration and simultaneously exacerbated the formation of secondary aerosols. The significant increase in pollutants in the Weinan area in winter is primarily caused by man-made emissions. Vehicle exhaust emissions during work hours also accumulate under the influence of adverse meteorological factors, reducing visibility and causing great harm to human health. Weinan is dominated by the crop industry, but the winter haze is serious. Except for coal burning, straw burning, automobile exhaust, and soot gas emissions in winter, the weather conditions in Weinan are unfavourable to the evacuation of haze, which leads to particularly serious winter pollution. Meteorological factors and conditions are difficult to change. The rapid increase of $PM_{2.5}$ concentration in Weinan is primarily due to the discharge of local pollutants and local topography, particularly the meteorological conditions during the subsequent severe pollution. Generally, environmental weather conditions play an important role in $PM_{2.5}$ pollution. In addition to local emission control, our results indicated that attention should be paid to the contribution of environmental and meteorological conditions to provide an effective and accurate analysis of air pollution control in Weinan area, which will help achieve better results. Government departments must strengthen management and strictly prohibit the discharge of pollutants that do not meet the standards to reduce the discharge of pollutants. Furthermore, citizens must strengthen their awareness of protecting the environment and improve the quality of urban life.

Data Availability

The data that support the findings of this study are available from the corresponding author upon reasonable request.

Conflicts of Interest

The authors declare that they have no conflicts of interest.

Authors' Contributions

Yuanyuan Meng was responsible for the methodology, investigation, and writing the original draft. Wan Long Sun provided constructive suggestions for improving the article. All authors contributed to the interpretation of the results and the improvement of this paper.

References

[1] A. J. Cohen, M. Brauer, R. Burnett et al., "Estimates and 25-year trends of the global burden of disease attributable to ambient air pollution: an analysis of data from the Global Burden of Diseases Study 2015," *The Lancet*, vol. 389, no. 10082, pp. 1907–1918, 2017.

[2] J. J. West, A. Cohen, F. Dentener et al., "What we breathe impacts our health: improving understanding of the link between air pollution and health," *Environmental Science and Technology*, vol. 50, no. 10, pp. 4895–4904, 2016.

[3] G. Q. Fu, W. Y. Xu, R. F. Yang, J. B. Li, and C. S. Zhao, "The distribution and trends of fog and haze in the North China Plain over the past 30 years," *Atmospheric Chemistry and Physics*, vol. 14, no. 21, pp. 11949–11958, 2014.

[4] H. Fu and J. Chen, "Formation, features and controlling strategies of severe haze-fog pollutions in China," *The Science of the Total Environment*, vol. 578, pp. 121–138, 2017.

[5] X. J. Zhao, P. S. Zhao, J. Xu et al., "Analysis of a winter regional haze event and its formation mechanism in the North China Plain," *Atmospheric Chemistry and Physics*, vol. 13, 2013.

[6] G. J. Zheng, F. K. Duan, Y. L. Ma et al., "Exploring the severe winter haze in Beijing (preprint)," *Atmospheric Chemistry and Physics*, vol. 15, 2014.

[7] L. Liu, X. Ma, W. Wen, C. Sun, and J. Jiao, "Characteristics and potential sources of wintertime air pollution in Linfen, China," *Environmental Monitoring and Assessment*, vol. 193, no. 5, p. 252, 2021.

[8] Y. Ding and Y. Liu, "Analysis of long-term variations of fog and haze in China in recent 50 years and their relations with atmospheric humidity," *Science China Earth Sciences*, vol. 57, no. 1, pp. 36–46, 2014.

[9] X. Zhang, J. Sun, Y. Wang et al., "Factors contributing to haze and fog in China," *Chinese Science Bulletin*, vol. 58, pp. 1178–1187, 2013.

[10] W. Dai, J. Q. Gao, B. Wang, and F. Ouyang, "Statistical analysis of weather effects on PM2.5," *Advanced Materials Research AMR 610–613*, vol. 610-613, pp. 1033–1040, 2012.

[11] Y. Liu, C. J. Paciorek, and P. Koutrakis, "Estimating regional spatial and temporal variability of PM 2.5 concentrations using satellite data, meteorology, and land use information," *Environmental Health Perspectives*, vol. 117, no. 6, pp. 886–892, 2009.

[12] G. W. Fuller, D. C. Carslaw, and H. W. Lodge, "An empirical approach for the prediction of daily mean PM10 concentrations," *Atmospheric Environment*, vol. 36, no. 9, pp. 1431–1441, 2002.

[13] L. Jian, Y. Zhao, Y.-P. Zhu, M.-B. Zhang, and D. Bertolatti, "An application of ARIMA model to predict submicron particle concentrations from meteorological factors at a busy roadside in Hangzhou, China," *The Science of the Total Environment*, vol. 426, pp. 336–345, 2012.

[14] M. Hu, L. Jia, J. Wang, and Y. Pan, "Spatial and temporal characteristics of particulate matter in Beijing, China using the Empirical Mode Decomposition method," *The Science of the Total Environment*, vol. 458–460, pp. 70–80, 2013.

[15] Y. C. Miao, Y. J. Zheng, S. Wang, and S. H. Liu, "Recent advances in, and future prospects of, research on haze formation over Beijing-Tianjin-Hebei, China," *Climatic and Environmental Research*, vol. 20, no. 3, pp. 356–368, 2015.

[16] L. Wang, N. Zhang, Z. Liu, Y. Sun, D. Ji, and Y. Wang, "The influence of climate factors, meteorological conditions, and boundary-layer structure on severe haze pollution in the beijing-tianjin-hebei region during january 2013," *Advances in Meteorology*, vol. 2014, pp. 1–14, 2014.

[17] X. Chen, S. Lai, Y. Gao et al., "Reconstructed light extinction coefficients of fine particulate matter in rural guangzhou, Southern China," *Aerosol Air Qual. Res*, vol. 16, pp. 1981–1990, 2016.

[18] X. Chen, L. Yin, Y. Fan et al., "Temporal evolution characteristics of PM2.5 concentration based on continuous wavelet transform," *The Science of the Total Environment*, vol. 699, Article ID 134244, 2020.

[19] J. Morlet, G. Arens, E. Fourgeau, and D. Glard, "Wave propagation and sampling theory-Part I: complex signal and scattering in multilayered media," *Geophysics*, vol. 47, no. 2, pp. 203–221, 1982.

[20] W. Zheng, X. Li, L. Yin et al., "Wavelet analysis of the temporal-spatial distribution in the Eurasia seismic belt," *International Journal of Wavelets, Multiresolution and Information Processing*, vol. 15, no. 3, Article ID 1750018, 2017.

[21] A. Grinsted, J. C. Moore, and S. Jevrejeva, "Application of the cross wavelet transform and wavelet coherence to geophysical time series," *Nonlinear Processes in Geophysics*, vol. 11, no. 5/6, pp. 561–566, 2004.

[22] A. C. Furon, C. Wagner-Riddle, C. R. Smith, and J. S. Warland, "Wavelet analysis of wintertime and spring thaw CO2 and N2O fluxes from agricultural fields," *Agricultural and Forest Meteorology*, vol. 148, no. 8-9, pp. 1305–1317, 2008.

[23] M. Farge, "Wavelet transforms and their applications to turbulence," *Annual Review of Fluid Mechanics*, vol. 24, no. 1, pp. 395–458, 1992.

[24] P. Abry and D. Veitch, "Wavelet analysis of long-range-dependent traffic," *IEEE Transactions on Information Theory*, vol. 44, no. 1, pp. 2–15, 1998.

[25] J. Allegrini and J. Carmeliet, "Coupled CFD and building energy simulations for studying the impacts of building height topology and buoyancy on local urban microclimates," *Urban Climate*, vol. 21, pp. 278–305, 2017.

[26] G. Guo, Z. Wu, R. Xiao, Y. Chen, X. Liu, and X. Zhang, "Impacts of urban biophysical composition on land surface temperature in urban heat island clusters," *Landscape and Urban Planning*, vol. 135, pp. 1–10, 2015.

[27] K. W. Oleson, G. B. Anderson, B. Jones, S. A. McGinnis, and B. Sanderson, "Avoided climate impacts of urban and rural heat and cold waves over the U.S. using large climate model ensembles for RCP8.5 and RCP4.5," *Climatic Change*, vol. 146, no. 3-4, pp. 377–392, 2018.

[28] A. B. Besir and E. Cuce, "Green roofs and facades: a comprehensive review," *Renewable and Sustainable Energy Reviews*, vol. 82, pp. 915–939, 2018.

[29] C. Cao, X. Lee, S. Liu et al., "Urban heat islands in China enhanced by haze pollution," *Nature Communications*, vol. 7, no. 1, p. 12509, 2016.

[30] J. Feng, M. Hu, C. K. Chan et al., "A comparative study of the organic matter in PM2.5 from three Chinese megacities in three different climatic zones," *Atmospheric Environment*, vol. 40, no. 21, pp. 3983–3994, 2006.

[31] P. Wu, Y. Ding, and Y. Liu, "Atmospheric circulation and dynamic mechanism for persistent haze events in the Beijing-Tianjin-Hebei region," *Advances in Atmospheric Sciences*, vol. 34, no. 4, pp. 429–440, 2017.

[32] X. Dong, D. Liu, and S. Gao, "Seasonal variations of atmospheric heterocyclic aromatic amines in Beijing, China," *Atmospheric Research*, vol. 120-121, pp. 287–297, 2013.

[33] B. Liu, N. Song, Q. Dai et al., "Chemical composition and source apportionment of ambient PM2.5 during the non-heating period in Taian, China," *Atmospheric Research*, vol. 170, pp. 23–33, 2016.

[34] Y. Li, S. Zhou, M. Hoffmann, G. Kumar, and M. Palmisano, "Modeling and simulation to probe the pharmacokinetic disposition of Pomalidomide R- and S-enantiomers," *Journal of Pharmacology and Experimental Therapeutics*, vol. 350, no. 2, pp. 265–272, 2014.

[35] D. E. Day and W. C. Malm, "Aerosol light scattering measurements as a function of relative humidity: a comparison between measurements made at three different sites," *Atmospheric Environment*, vol. 35, no. 30, pp. 5169–5176, 2001.

[36] T. Hussein, A. Karppinen, J. Kukkonen et al., "Meteorological dependence of size-fractionated number concentrations of urban aerosol particles," *Atmospheric Environment*, vol. 40, no. 8, pp. 1427–1440, 2006.

[37] J. A. Salmond and I. G. McKendry, "A review of turbulence in the very stable nocturnal boundary layer and its implications for air quality," *Progress in Physical Geography: Earth and Environment*, vol. 29, no. 2, pp. 171–188, 2005.

[38] M. Hallquist, J. C. Wenger, U. Baltensperger et al., "The formation, properties and impact of secondary organic aerosol: current and emerging issues," *Atmospheric Chemistry and Physics*, vol. 82, 2009.

[39] C. J. Hennigan, M. H. Bergin, J. E. Dibb, and R. J. Weber, "Enhanced secondary organic aerosol formation due to water uptake by fine particles," *Geophysical Research Letters*, vol. 35, no. 18, Article ID L18801, 2008.

[40] H. Kang, B. Zhu, J. Su, H. Wang, Q. Zhang, and F. Wang, "Analysis of a long-lasting haze episode in Nanjing, China," *Atmospheric Research*, vol. 120-121, pp. 78–87, 2013.

[41] F. Environmental Protection Agency, *Visibility in mandatory federal class I areas (1994–1998), Report, Off. of Air Qual. Plan. and Stand*, Research Triangle Park, NC, USA, 2001.

[42] R. B. Husar, J. M. Holloway, D. E. Patterson, and W. E. Wilson, "Spatial and temporal pattern of eastern U.S. haziness: a summary," *Atmospheric Environment (1967)*, vol. 15, no. 10-11, pp. 1919–1928, 1981.

[43] D. S. Kaul, T. Gupta, S. N. Tripathi, V. Tare, and J. L. Collett, "Secondary organic aerosol: a comparison between foggy and nonfoggy days," *Environmental Science and Technology*, vol. 45, no. 17, pp. 7307–7313, 2011.

[44] W. L. Chameides, R. W. Lindsay, J. Richardson, and C. S. Kiang, "The role of biogenic hydrocarbons in urban photochemical smog: atlanta as a case study," *Science*, vol. 241, no. 4872, pp. 1473–1475, 1988.

[45] S. Sillman, "The relation between ozone, NOx and hydrocarbons in urban and polluted rural environments," *Atmospheric Environment*, vol. 33, 1999.

[46] F. Ahamad, M. T. Latif, R. Tang, L. Juneng, D. Dominick, and H. Juahir, "Variation of surface ozone exceedance around Klang Valley, Malaysia," *Atmospheric Research*, vol. 139, pp. 116–127, 2014.

[47] N. R. Awang, M. Elbayoumi, N. A. Ramli, and A. S. Yahaya, "Diurnal variations of ground-level ozone in three port cities in Malaysia," *Air Quality, Atmosphere & Health*, vol. 9, no. 1, pp. 25–39, 2016.